12 Annual Conference of the Materials Research Society of Serbia, Herceg Novi, Montenegro, September 6–10, 2010

Low Temperature Magnetic Properties of $Pr_{0.7}(Ca,Sr)_{0.3}CoO_3$ Oxides

I.G. Deac*, A. Vlădescu, I. Balasz, A. Tunyagi and R. Tetean

Faculatea de Fizica, Universitatea Babes-Bolyai, Str. Kogalniceanu 1,Cluj-Napoca 400084, Romania

We have investigated magnetic and magnetocaloric properties of $Pr_{0.7}(Ca_{1-x}Sr_x)_{0.3}CoO_3$, when the average size of the interpolated cation was changed. $Pr_{0.7}Ca_{0.3}CoO_3$ has an orthorhombic *Pnma* symmetry and it shows a magnetic cluster-glass behavior below 70 K. When Sr partially replaces Ca in this compound, its magnetic properties are improved, and it begins to have ferromagnetic-like behavior. The magnetic transition temperature, gradually, increases with increasing Sr content, up to 170 K, for $x = 1$. The electrical conduction also improved when Sr content increased. All the samples show negative magnetoresitance. Magnetic entropy change ΔS_M was estimated from isothermal magnetization data. We have found that it had higher values for the samples with $x > 0.5$, around 1 J/kg K for $\Delta B = 4$ T, with reasonable good relative cooling power.

PACS: 75.47.Lx, 75.30.Kz, 75.30.Sg, 73.43.Qt

1. Introduction

The ABO_3-type transition metal oxides display remarkable magnetic and transport properties of interest for basic science as well as for technical applications (for use in solid oxide fuel cell, chemical reactors, gas separation membranes and many other applications) [1]. Doped cobaltite perovskites $Ln_{1-x}A_xCoO_3$ (Ln= La, rare earth and A = Ca, Sr, Ba), have recently attracted much attention due to their unique feature to change the spin-state of the Co^{3+}(low-spin LS: $t_{2g}^6e_g^0$, intermediate-spin IS: $t_{2g}^5e_g^1$, high-spin HS: $t_{2g}^4e_g^2$) and Co^{4+}(LS: $t_{2g}^5e_g^0$, IS: $t_{2g}^4e_g^1$, HS: $t_{2g}^3e_g^2$) ions. The existence of the spin state change indicates that the difference of the electronic energies, δE, between these spin states is rather small, since the crystal field splitting of the Co-*d*states and Hund's rule coupling energy are comparable for these compounds. With increasing temperature some of Co ions are progressively converted to IS or to HS state due to the small difference between Hund and crystal field energies that allows the thermal excitation of t_{2g} electrons on e_g levels [2]. This aspect was largely studied on $LaCoO_3$ and it was found in some other cobaltites like $PrCoO_3$ and $NdCoO_3$, showing that the transition temperature varies as a function of the rare earth ion in the $LnCoO_3$ series [2, 3]. We can control the physical properties of Co oxides by controlling the value of δE, for example, by changing the ionic radius $\langle r_A \rangle$ of Ln, by doping A-type ions at Ln ion site. If Sr (for example) substitutes for Ln in these Co perovskites, a transition from paramagnetic phase to the ferromagnetic one takes place with increasing doping content, at about 20% [3]. $PrCoO_3$ shows paramagnetic behavior down to 5 K [4]. The compound $Pr_{0.7}Sr_{0.3}CoO_3$ was found to be ferromagnetic (below 170 K) and metallic down to about 100 K, and then semiconductor at lower temperatures [4–6]. $Pr_{0.7}Ca_{0.3}CoO_3$ has a seminconductor–like (in the whole temperature range) and a magnetic cluster-glass behavior [6–9] below 70 K. The physical properties of these compounds will depend on the average size of the A-site (Ln^{3+} and A^{2+}) cations, $\langle r_A \rangle = \sum x_i r_i$ (where x_i is the fractional occupancy of A-site ions, and r_i is the corresponding ionic radius) [10, 11].

When a magnetic field is applied adiabatically on a magnetic material the temperature of the material rises, and when the field is removed the temperature decreases since the magnetic moments of the atoms become reoriented. This phenomenon is known as "magnetocaloric effect" (MCE). The latter effect is an isothermal magnetic entropy change or an adiabatic temperature change of a magnetic material upon application of a magnetic field [12]. The compounds that undergo temperature-driven paramagnetic to ferromagnetic transitions show relatively large MCE. The mixed-valency perovskites have attracted renewed interest in research due to their potential application as active magnetic materials in magnetic refrigeration techniques. Most of the studies were done on the so-called "colossal magnetoresistive manganites" [13]. Doped perovskites cobaltites have proven very useful for the study of this phenomenon, since they also have sharp paramagnetic to ferromagnetic-like transition and they are tunable by adjustment of the doping concentration. Like manganites [14], the different forms of cobaltites exhibit interesting phenomena including spin, charge and orbital ordering, electronic phase separation, insulator-metal transition, large thermoelectric power at low temperature [1–3].

In order to do a systematic analysis of how the electrical and magnetic properties can be tuned by doping, the series of cobaltites $Pr_{0.7}(Ca_{1-x}Sr_x)_{0.3}CoO_3$ was studied

* corresponding author; e-mail: ideac@phys.ubbcluj.ro

when $\langle r_A \rangle$ gradually changes , in fine steps, from 1.305 Å (for $x = 0$) to 1.335 Å (for $x = 1$). The perovskite A-site is coordinated by 12 O^{-2} ions and we used the ionic radii $R(Pr^{3+}) = 1.29$ Å, $R(Ca^{2+}) = 1.34$ Å and $R(Sr^{2+}) = 1.44$ Å [14].

2. Experimental details

The $Pr_{0.7}(Ca_{1-x}Sr_x)_{0.3}CoO_3$ compounds with $x = 0$, 0.2, 0.5, 0.7, 0.8, 0.95, and 1 were prepared by conventional solid-state reaction. The mixtures of the respective oxides were calcined at 900 ℃ and sintered in air at 1180 ℃ for 24 hours, with intermediate grindings. The powder x-ray diffraction patterns were recorded by using a Bruker D8 Advance AXS diffractometer with Cu K_α radiation. Data were refined by the Rietveld method using the program FULLPROF. A cryogen free VSM 12 T magnetometer (Cryogenic Ltd.) was used for magnetization and ac susceptibility measurements in the temperature range 5 - 300 K and up to 12 T. The temperature dependent magnetization, $M(T)$, was recorded on warming in zero field-cooled (ZFC) and field-cooled (FC) modes. The resistivities were measured in another cryogen free magnet cryostat CFM-7 T (Cryogenic Ltd.) by the four-probe technique, in the temperature range from 5 to 300 K and magnetic fields up to 7 T.

The magnetocaloric effect (MCE) can be estimated by means of the magnetic entropy change $\Delta S_M(T, H_0)$. In order to do this, we measured the isothermal $M-H$ curves under different temperatures using the thermodynamic relation relation [12] (for second order phase transitions):

$$\Delta S_M(T, H_0) = S_M(T, H_0) - S_M(T, 0)$$
$$= \frac{1}{\Delta T} \int_0^{H_0} [M(T + \Delta T, H) - M(T, H)] \mathrm{d}H$$

where ΔT is the temperature increment between measured magnetization isotherms ($\Delta T = 5$K for our data). Generally, the important index for selecting magnetic refrigerants is based on the cooling power per unit volume, namely, the relative cooling power (RCP):

$$\mathrm{RCP}(S) = -\Delta S_M(\max)\delta T_{FWHM}$$

where $\Delta S_M(\max)$ is the maximum magnetic entropy change and δT_{FWHM} is the full width at half maximum of the magnetic entropy change curve [12, 13, 15].

3. Results and discussion

All the samples are single phase without detectable secondary phase, within the sensitivity limits of the experiment, and they have orthorhombic *Pnma* type structure. The x-ray diffraction pattern for a typical $x = 0.5$ sample is shown in Fig. 1. Detailed results of the structural refinements are listed in Table.

When Ca^{2+} ions are substituted by Sr^{2+} ions, which have larger ionic radius, the average ionic radius of A-site $\langle r_A \rangle$ increases with the increase in Sr concentration. As

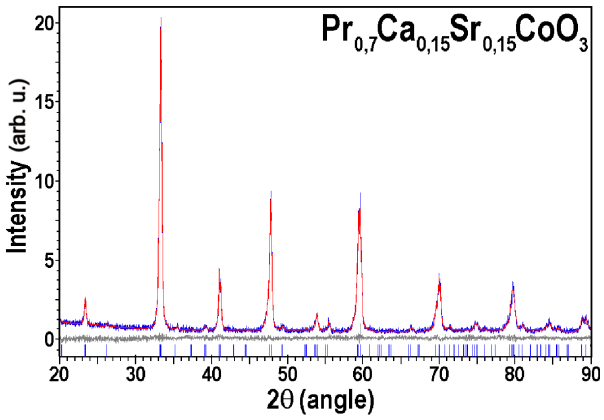

Fig. 1. Rietveld refinement plot of the x-ray diffraction data for the sample with $x = 0.5$. Observed, calculated, and difference profiles are plotted on the same scale. The Bragg peaks are indicated by tick marks.

can be seen from Table, the principal effect of decreasing $\langle r_A \rangle$ is to lower the Co-O-Co bond angle away from 180 ° , and the effect will be to reduce the overlap of the Co and O orbitals. The substitution of Sr for Ca will expand the unit cell and will make it more symmetrical.

The rapid increase of M around T_C signals the phase transition from a paramagnetic to an ordered state. The temperature dependence of magnetization is strongly dependent on magnetic history starting from a temperature just below T_C to the lowest temperature with a bifurcation between ZFC and FC data at an irreversibility temperature T_{irr}, as shown in Fig. 2 for the samples with $x = 0$, 0.2, 0.5 and 0.95. The FC branches of the temperature dependence of magnetizations exhibit typical ferromagnetic behavior for the samples with $x > 0$. The ferromagnetic T_C's of our samples, are estimated from the common inflection points of both $M_{ZFC}(T)$ and $M_{FC}(T)$ curves and they are indicated in Table. The hysteresis loops indicate that all the samples have ferromagnetic-like behavior, as shown in Fig. 2 for the sample with $x = 0.5$. The width of the hysteresis loop decreases markedly with increasing temperature.

The difference in the magnetization behavior between the FC and ZFC regimes reflects the energy involved in the alignment of magnetic domains in the samples suggesting that the applied field (0.1 T) is lower than the coercive field. The bifurcation between $M_{ZFC}(T)$ and $M_{FC}(T)$ curves is typical for doped cobaltites [3–15, 16]. No saturation was seen in $M(H)$ curves for any of the samples, even up to 12 T. Such a behavior suggests the coexistence of a dominant ferromagnetic phase together with a non-ferromagnetic one, i.e., a phase separation scenario. We also include in this non-ferromagnetic phase, the paramagnetic contribution from the Pr^{3+} ions.

The ferromagnetic fraction grows with increasing x for the samples with $x > 0$. For the sample with $x = 0$, the increase of the magnetization takes place slowly with decreasing temperature in a very large temperature range,

suggesting a broad distribution of T_C's. $Pr_{0.7}Ca_{0.3}CoO_3$ has a behavior that is unlike of ferromagnets and is somewhat comparable to that of frustrated systems. The shape of the $M(T)$ curve for this sample was rather complex, not typical for pure ferromagnets, with a maximum in M_{ZFC}(T) at $T_f \sim 16$ K and a frequency dependent maximum in ac susceptibility (not shown), both in the real part $\chi'(T)$ and in the imaginary part $\chi''(T)$ [6, 8].

TABLE

Quantitative data for the $Pr_{0.7}(Ca_{1-x}Sr_x)_{0.3}CoO_3$ compounds

x	0	0.2	0.5	0.7	0.8	0.95	1
a [Å]	5.3526	5.3855	5.4024	5.4127	5.4201	5.4265	5.4268
b [Å]	7.5714	7.5754	7.5854	7.5915	7.5975	7.6009	7.6039
c [Å]	5.3526	5.3576	5.3624	5.3673	5.3704	5.3717	5.3738
V [Å^3]	217.427	218.579	219.751	220.551	221.156	221.569	221.901
$\langle r_A \rangle$	1.305	1.311	1.320	1.326	1.329	1.333	1.335
Co–O1–Co	145.32	150.15	152.65	155.89	156.83	157.07	157.22
Co–O2–Co	148.35	153.22	154.09	157.17	157.87	158.09	165.10
O1-Co-O2	119.72	112.23	110.27	107.99	107.49	106.99	84.58
T_C [K]	—	68	116	125	134	162	168

The ferromagnetic transition temperatures increase with increasing Sr content in the samples. The cluster-glass behavior of the parent compound $Pr_{0.7}Ca_{0.3}CoO_3$ is suppressed with increase in the substituent Sr ion concentrations. It seems that, the introduction of strontium in the distorted perovskite cages locally hinders the distortion of the structure. In this way, more symmetric domains will develop around the Sr^{2+} ion. This is the so-called "counter-distortion" effect [11], previously seen in manganites [17] It is believed that, as well as in the case of manganites, magnetic interaction of the type of double exchange between Co^{3+} and Co^{4+} ions is responsible for the ferromagnetism of cobaltites [2, 3]. Usually, the complex spin-charge-orbital-lattice coupling results in a cluster glass behavior that is a sign of magnetic phase separation in the system, i.e. ferromagnetic order but with a possible coexistence of superparamagnetic clusters (in our case) [5, 7, 16].

In order to evaluate the MCE, the isothermal magnetization curves of the samples were measured with a field step of 1T in a range of 0–4T and a temperature step of 5 K over a range of temperatures around T_C. Such families of $M(H)$ curves are shown in Fig. 3(a) for the sample with $x = 0.8$, as an example. To study the nature of the magnetic transition we built the Arrot plot and we used the Banerjee criterion [18]. In Fig. 3(b) we plot the M^2 versus M/H curves (Arrot plot) where a positive slope is clearly seen in all the M^2 range, indicating that the phase transition is second order [18]. The second-order magnetic transition at T_C induces a smaller MCE but with a distribution over a broader temperature range, thus resulting in a larger RCP.

The temperature dependences of magnetic entropy change in 1, 2, 3 and 4T external applied fields for the compound with $x = 0.95$, and 0.2 are plotted in Fig. 4, as examples. The maximum values of entropy change occur almost around the transition temperatures for all the compounds. We cannot talk about a significant MCE for the sample with $x = 0$ since, we have a low magnitude of magnetization and a broaden transition, with a distribution of T_C's that lead to negligible values for $(\partial M(T,H)/\partial T)_H$.

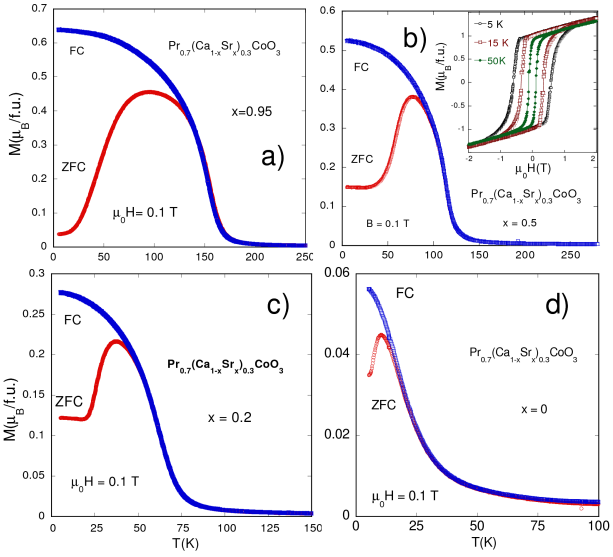

Fig. 2. Field cooled (FC) and zero field cooled (ZFC) magnetization of $Pr_{0.7}(Ca_{1-x}Sr_x)_{0.3}CoO_3$ as a function of temperature, measured in 0.1 T. For a) $x = 0.9$, b) $x = 0.5$, (in inset: the hysteresis loops at 5, 15 and 50 K), c) $x = 0.2$ and d) $x = 0$.

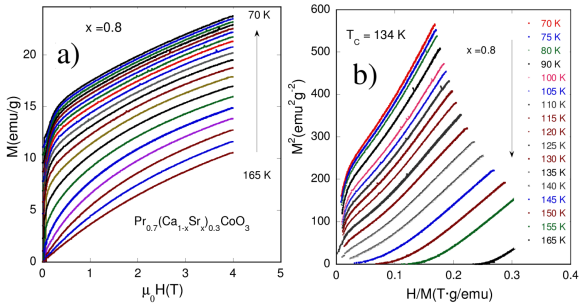

Fig. 3. (a). Isothermal magnetization curves taken at different fixed temperatures between 70 and 165K for the $Pr_{0.7}(Ca_{0.2}Sr_{0.8})_{0.3}CoO_3$ cobaltite. (b) Arrot plot obtained from measured M vs. H isotherms, for the sample with $x = 0.8$.

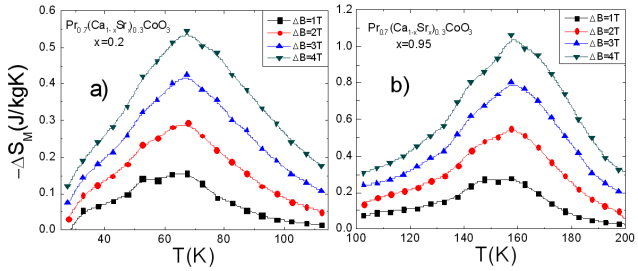

Fig. 4. The temperature dependences of the magnetic entropy change for the samples with $x = 0.2$ (a) and $x = 0.95$ (b), in $\Delta B = 1$, 2, 3 and 4 T.

The maximum value of the entropy change, $-\Delta S_M(\max)$, is 1.065 J/kg K in 4 T, for the sample with $x = 0.95$ and it decreases linearly to 0.28 J/kg K when the field goes from 4 to 1 T. The values of the maximum of the entropy change, $-\Delta S_M(\max)$, are almost the same for $x > 0.5$, while the widths at the half maximum gradually increase from 51 K, for $x = 1$ to 63 K for $x = 0.5$ in 4 T. The relative cooling power, RCP is maximum for the sample with $x = 0.8$ being 54.9 J/kg for $\Delta B = 4$ T, 44.8 J/kg for $\Delta B = 3$ T , 30.2 J/kg for $\Delta B = 2$ T and 15.7 J/kg for $\Delta B = 1$ T. The sample with $x = 0.5$ has RCP's as 53.5 J/kg , 41.6 J/kg, 29.4 J/kg and 15.2 J/kg, respectively. By using these (Ca,Sr) dopings, with $x > 0.2$, the relative cooling powers will not change very much, but they could be used in different temperature ranges. These values for RCP are somewhat smaller than those obtained in doped manganite perovskites but they are high enough for technical interest.

The samples have semiconducting behavior at low temperatures, in spite of their very low values of the electrical resistivity. In Fig. 5 is described the temperature dependence of resistivity in zero applied magnetic field for the samples with $x = 0.2$, 0.5, 0.8 and 0.95 (for clarity). The samples with $x > 0.5$ have metallic behavior down to about 100 K, and then they have semiconductor behavior ($\mathrm{d}\rho/\mathrm{d}T < 0$) at lower temperatures, probably, due to a grain boundary effect [19]. The samples with higher Ca content have semiconductor behavior in the whole temperature range. It can be seen that the value of the resistivity decreases with increasing Sr content in the samples. This behavior suggests, again, that more symmetric domains will develop around the Sr^{2+} ions allowing a better overlapping of the Co and O orbitals. There is no signature of the magnetic phase transition on the temperature dependence of resistivity. This decoupling of magnetization and transport is unusual in perovskites, where the double exchange mechanism presumes a link between electron hopping and magnetic moments alignment [1, 14]. A possible explanation for this can reside in the electron scattering mechanism at the grain boundaries, which can mask the change in the electrical conduction due to the magnetic phase transition [19].

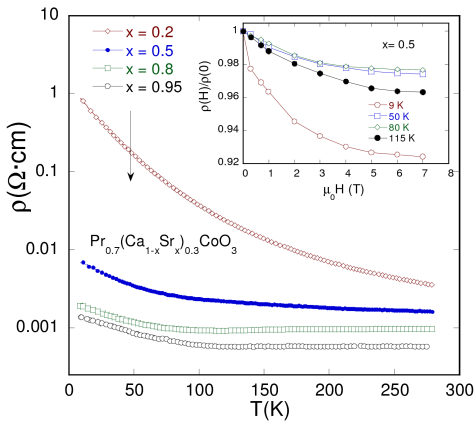

Fig. 5. The temperature dependence of electrical resistivity in zero applied magnetic field, for the samples with $x = 0.2$, 0.5, 0.8 and 0.95. In inset: $\rho(H)/\rho(0)$ measured at 9 K, 50 K, 80 K and 150 K for the sample with $x = 0.95$.

All the samples showed negative magnetoresistence. For the samples with high Ca content the magnetoresitence is maximum at the lowest temperature and in 7 T, as can be seen in the inset of Fig. 5. In this case, the magnetoresitance $MR = 1-\rho(H)/\rho(0)$ can be about 7.6%, at 9 K and 7 T, for the sample with $x = 0.5$. For the other samples, MR at 9 K and 7 T is not higher than 3%. Thus, the larger MR observed for these samples at 9 K can be interpreted as tunnelling magnetoresistance (TMR) effect due to the increase of the intergrain insulating barriers, as it was found in some other transition metal oxides [20]. A better coupling between transport and magnetic properties can be found in the sample with $x = 0.95$, where the maximum MR is about 5% in 7 T and 150 K, while for the sample with $x = 1$ it was about 3.4% close to the magnetic transition.

The decrease of resistivity and the enhancement of the magnetic properties with increasing Sr content in the samples suggest that these properties can be correlated, as in the case of the manganite perovkites where

the double exchange interaction improves the electrical conduction. The magnetotransport data can be described in terms of percolative transport through some ferromagnetic-like, metallic regions, in the presence of grain boundary scatterings [19, 20].

4. Conclusions

High-quality samples of $Pr_{0.7}(Ca_{1-x}Sr_x)_{0.3}Co_xO_3$ (x = 0, 0.2, 0.5, 0.8, 0.95, and 1) were prepared by standard ceramic reaction, and their magnetic and electrical properties were investigated. All the compounds crystallize in an orthorhombic structure. The samples with $x > 0$ show ferromagnetic-like behavior (ferromagnetic order but with a possible coexistence of superparamagnetic clusters) below a transition temperature, that decreases with decreasing Sr content in the samples. $Pr_{0.7}Ca_{0.3}CoO_3$ has cluster-glass behavior, with no long range magnetic order. When Sr partially replaces Ca in this system, the cluster-glass behavior is suppressed and the magnetism is enhanced. Similarly, the electrical conduction is improved with increasing Sr content in the samples. All the samples have negative magnetoresistance at low temperatures. The electrical conduction is percolative and controlled by grain boundary effects. The maximum magnetic entropy change, $-\Delta S_M(\max)$, for the samples with $x > 0.5$, is around 1 J/kg K, while RCP is around 54 J/kg, for $\Delta B = 4$ T. By (Ca,Sr) doping in this system we can obtain rather high cooling powers in various temperature ranges, with reasonably good magnetocaloric values.

Acknowledgments

This work was supported by the grant PNII-IDEI code 2590/2008 of CNCSIS-UEFISCSU, Romania.

References

[1] J.B. Goodenough, *Rep. Prog. Phys.* **67,** 1915 (2004).

[2] M.A. Señarís-Rodríguez, J.B. Goodenough, *J. Solid State Chem.* **118**, 323 (1995).

[3] J.–Q. Yan, J.–S. Zhou, J.B. Goodenough, *Phys. Rev. B* **69**, 134409 (2004).

[4] H.W. Brinks, H. Fjellvag, A. Kjekshus, B.C. Hauback, *J. Solid State Chem.* **147**, 464 (1999).

[5] C. Leighton, D.D. Stauffer, Q. Huang, Y. Ren, S. El-Khatib, M.A. Torija, J. Wu, J.W. Lynn, L. Wang, N.A. Frey, H. Srikanth, J.E. Davies, Kai Liu, J.F. Mitchell, *Phys. Rev. B* **79**, 214420 (2009).

[6] I.G. Deac, A. Vlădescu, I. Balasz, A. Tunyagi, R. Tetean, *Int. J. Mod. Phys. B* **24**, 762 (2010).

[7] A.K. Kundu, P. Nordblad, C.N.R. Rao, *J. Solid State Chem.* **179**, 923 (2006).

[8] I.G. Deac, R. Tetean, D. Andreica, E. Burzo, *IEEE Trans. Magn.* **44**, 2922 (2008).

[9] T. Fujita, T. Miyashita, Y. Yasui, Y. Kobayashi, M. Sato, E. Nishibori, M. Sakata, T. Adachi, Y. Ohishi, M. Takata *J. Phys. Soc. Jpn.* **73**, 1987 (2004).

[10] J.P. Attfield, *Cryst. Eng.* **5**, 427 (2002).

[11] B. Raveau, *Phil. Trans. R. Soc. A* **366**, 83 (2008).

[12] A.M. Tishin, Y.I. Spichkin, *The Magnetocaloric Effect and Its Applications*, Institute of Physics, Bristol 2003.

[13] M.H. Phan, S.C. Yu, *J. Magn. Magn. Mater.* **308**, 325 (2007).

[14] Y. Tokura, *Rep. Prog. Phys.* **69,** 797 (2006).

[15] V.K. Sharma, M.K. Chattopadhyay, S.B. Roy, *J. Phys. D: Appl. Phys.* **40**, 1869 (2007).

[16] H.M. Aarbogh, J. Wu, L. Wang, H. Zheng, J.F. Mitchell, C. Leighton, *Phys. Rev. B* **74,** 134408 (2006).

[17] D. Zhu, P. Cao, W. Liu, X. Ma, A. Maignan, B. Raveau, *Materials Letters* **61**, 617 (2007).

[18] S.K. Banerjee, *Phys. Lett.* **12,** 16 (1964).

[19] M. Ziese, *Rep. Prog. Phys.* **65,**143 (2002).

[20] A.K. Kundu, B. Raveau, arXiv:1005.5426v1 [cond-mat.mtrl-sci] (2010).